

# The easy axis of the magnetic response of the conduction electrons of yttrium and rare earths

V.Thakor<sup>†</sup>, J.B.Staunton<sup>†</sup>, J.Poulter<sup>‡</sup>, S.Ostanin<sup>†</sup>, B.Ginatempo<sup>¶</sup>, and Ezio Bruno<sup>¶</sup>

<sup>†</sup> *Department of Physics, University of Warwick, Coventry CV4 7AL, U.K.*

<sup>‡</sup> *Department of Mathematics, Faculty of Science, Mahidol University, Bangkok 10400, Thailand. and*

<sup>¶</sup> *Dipartimento di Fisica and Unita INFM, Universita di Messina, Italy*

(Dated: November 20, 2018)

We describe a scheme for first-principles calculations of the static, paramagnetic, spin susceptibility of metals with relativistic effects such as spin-orbit coupling included. This gives the direction for an applied modulated magnetic field to maximise its response. This *easy axis* depends on the modulation's wave-vector  $\mathbf{q}$ . For h.c.p. yttrium we find the peak response at a  $\mathbf{q} = (0, 0, 0.57)\pi/c$ , coincident with a Fermi surface nesting vector, to have an easy axis perpendicular to  $\mathbf{q}$ . This is consistent with the *helical* anti-ferromagnetic order found in many dilute rare earth-Y alloys. Conversely, the easy axis for the response to a uniform magnetic field lies along the c-axis. The conduction electrons' role in the canting of magnetic moments in *Gd-Y* alloys and other rare earth materials is mooted.

PACS numbers: 75.40Cx, 71.15Rf, 75.25+z, 71.20.Be, 71.20.Eh

Conduction electrons play an important role in the magnetism of rare earths. Specifically they determine the Ruderman-Kittel-Kasuya-Yosida (RKKY) indirect exchange interactions which connect the localised 4f magnetic moments of the materials. [1] The magnetic response of the conduction electrons, the wave-vector dependent susceptibility  $\chi(\mathbf{q})$ , governs the ordering of the moments. If the greatest value of  $\chi(\mathbf{q})$  is for  $\mathbf{q} = (0, 0, 0)$ , the moments order ferromagnetically. A peak for  $\chi(\mathbf{q})$  at some finite  $\mathbf{q}$ , on the other hand, signifies a more complicated magnetic structure with a modulation wave-vector equal to  $\mathbf{q}$ . In many of the heavier rare earths, e.g. Tb, Dy, Ho and Er the incommensurate anti-ferromagnetic (AF) ordered states, modulated along the c-axes of these h.c.p. crystalline elements, depend strongly on the Fermi surface topology of the conduction electrons. The salient part of the Fermi surface (FS) that causes this anisotropy is the *webbing* feature that contains flat parallel sheets perpendicular to the c-axis forming a strong nesting effect [2, 3].

The link between FS nesting and the  $\mathbf{q}$ -dependence of  $\chi(\mathbf{q})$  is well-known and has been explored by electronic structure calculations. [4] There is however another anisotropy in the interaction between the rare earth (RE) magnetic moments that we suggest is also traceable to  $\chi(\mathbf{q})$ . This comes from spin-orbit coupling effects on the conduction electrons and affects whether the localised moments lie perpendicular to the c-axis and thus form helical AF magnetic states or instead have components along the c-axis and order into b-axis modulated AF phases. Of course the anisotropic crystal field acting on the 4f-shell plays an important role in this aspect but the similarity between Gd alloys in which the crystal field effects are small and alloys of Dy, Tb, etc suggests a generic feature from the conduction electrons. This is the issue we address in this letter. We describe a 'first-principles' theoretical formalism for the magnetic

response of paramagnetic metals in which all relativistic effects such as spin-orbit coupling are included. For the first time the *easy axis* and its dependence upon wave-vector  $\mathbf{q}$  for the magnetic response can be calculated. In effect we elucidate a relativistic RKKY interaction. [5]

We present specific calculations of the magnetic response of the transition metal yttrium. With the same h.c.p. crystal structure and electronic configuration as the rare earths, apart from the f-electrons, it provides an excellent model for their conduction electrons. Much is being learnt about the magnetism of rare earths from the varied and complex magnetic structures that they form in multilayers with yttrium. [6] These range from canted, antiphase domain structure in *Gd/Y* multilayers to coherent, incommensurate magnetic helices found in *Dy/Y* and *Ho/Y* structures. The mediating role of the conduction electrons of Y for these rare earth magnetic interactions is crucial in these tailored systems. [7] High quality samples of yttrium are more easily come by than the heavy rare earths and recent experiments [8] have measured directly the 'webbing' feature of its Fermi surface that it has in common with several rare earths. Moreover the nature of the magnetic ordering of low concentrations of rare earth dopants in Y can be directly related to this study. [9, 10, 11]

We begin by considering a paramagnetic metal subjected to a small, external, inhomogeneous magnetic field,  $\delta\mathbf{b}^{ext}(\mathbf{r})$ , and obtain an expression for the induced magnetisation  $\delta\mathbf{m}(\mathbf{r})$ . We use relativistic density functional theory (RDFT) [12] to treat the interacting electrons of the system and derive an expression via a variational linear response approach [13, 14, 15]. Although there are a number of non-relativistic studies of this type [16] here we include relativistic effects and pay particular attention to the magnetic anisotropy of the response. From our RDFT starting point we make a Gordon decomposition of the current density [12] and retain

the spin-only part of the current, namely the spin magnetisation  $\mathbf{m}(\mathbf{r})$ . This results in a *spin-only* version of RDFFT. [12] in which the self-consistent solution of Kohn-Sham-Dirac equations is sought, i.e.

$$[c\tilde{\alpha}\cdot\hat{\mathbf{p}} + \tilde{\beta}mc^2 + \tilde{\mathbf{I}}V^{eff}[\rho, \mathbf{m}] - \tilde{\beta}\tilde{\boldsymbol{\sigma}}\cdot\mathbf{b}^{eff}[\rho, \mathbf{m}] - \varepsilon] \times G(\mathbf{r}, \mathbf{r}'; \varepsilon) = \tilde{\mathbf{I}}\delta(\mathbf{r} - \mathbf{r}') \quad (1)$$

which describes the motion of a single electron through effective fields and  $\tilde{\alpha}$  and  $\tilde{\beta}$  are Dirac  $4 \times 4$  matrices.  $G(\mathbf{r}, \mathbf{r}'; \varepsilon)$  is the one electron Greens function and the charge  $\rho(\mathbf{r})$  and magnetisation densities  $\mathbf{m}(\mathbf{r})$  can be written in terms of it i.e.

$$\rho(\mathbf{r}) = -Tr. \int d\varepsilon f(\varepsilon, \mu, T) \frac{Im}{\pi} G(\mathbf{r}, \mathbf{r}; \varepsilon)$$

$$\mathbf{m}(\mathbf{r}) = -Tr. \tilde{\beta}\tilde{\boldsymbol{\sigma}} \int d\varepsilon f(\varepsilon, \mu, T) \frac{Im}{\pi} G(\mathbf{r}, \mathbf{r}; \varepsilon) \quad (2)$$

where  $\mu$  is the chemical potential,  $T$  the temperature and  $f(\varepsilon, \mu, T)$  the Fermi-Dirac function. These expressions can be converted into sums over fermionic Matsubara frequencies  $\omega_n = i(2n + 1)\pi k_B T$  [17]. The effective potential  $V^{eff}[\rho, \mathbf{m}]$  consists of the usual combination of external potential (from the lattice of nuclei), the Hartree potential and functional derivative of exchange-correlation energy  $E_{xc}[\rho, \mathbf{m}]$  with respect to  $\rho$  whilst the effective magnetic field  $\mathbf{b}^{eff}[\rho, \mathbf{m}]$  is the sum of any external magnetic field (from magnetic impurities, for example) and the functional derivative of  $E_{xc}$  with respect to magnetisation. We use the local density approximation (LDA) [18] for  $E_{xc}$ . The leading relativistic effects contained in the Kohn-Sham-Dirac hamiltonian of eq.(1) are the well-known mass-velocity, Darwin and spin-orbit coupling effects.

If a small external field  $\delta\mathbf{b}^{ext}$  is applied along a direction  $\hat{\mathbf{n}}$  with respect to the crystal axes of a paramagnetic system, a small magnetisation,  $\delta\mathbf{m}(\mathbf{r})$ , and effective magnetic field,  $\delta\mathbf{b}^{eff}$  are set up. The effective magnetic field is given by  $\delta\mathbf{b}^{eff}[\rho(\mathbf{r}), \mathbf{m}(\mathbf{r})] = \delta\mathbf{b}^{ext}(\mathbf{r}) + I_{xc}(\mathbf{r})\delta\mathbf{m}(\mathbf{r})$  where  $I_{xc}(\mathbf{r})$  is the functional derivative of the effective exchange and correlation magnetic field (within the LDA) with respect to the induced magnetisation density. The Green's function satisfying equation (1) can be expanded in a Dyson equation in terms of the unperturbed Green's function,  $G_o(\mathbf{r}, \mathbf{r}'; \varepsilon)$  of the paramagnetic system ( $\delta\mathbf{b}^{eff} = 0$ ) and perturbation  $\tilde{\beta}\tilde{\boldsymbol{\sigma}}\cdot\delta\mathbf{b}^{eff}$  and the first order terms enable the magnetic response function to be obtained.

For a general crystal lattice with  $N_s$  atoms located at positions  $\mathbf{a}_l$  ( $l = 1, \dots, N_s$ ) in each unit cell, a lattice Fourier transform can be carried out over lattice vectors  $\{\mathbf{R}_i\}$ . This can be written

$$\chi^{\hat{\mathbf{n}}}(\mathbf{x}_l, \mathbf{x}'_{l'}, \mathbf{q}) = \chi_o^{\hat{\mathbf{n}}}(\mathbf{x}_l, \mathbf{x}'_{l'}, \mathbf{q}) + \sum_{l''}^{N_s} \int \chi_o^{\hat{\mathbf{n}}}(\mathbf{x}_l, \mathbf{x}''_{l''}, \mathbf{q}) I_{xc}(\mathbf{x}''_{l''}) \times \chi^{\hat{\mathbf{n}}}(\mathbf{x}''_{l''}, \mathbf{x}'_{l'}, \mathbf{q}) d\mathbf{x}''_{l''} \quad (3)$$

where the  $\mathbf{x}_l$  are measured relative to the positions of atoms centred on  $\mathbf{a}_l$ . The non-interacting susceptibility of the static unperturbed system is given by

$$\chi_o^{\hat{\mathbf{n}}}(\mathbf{x}_l, \mathbf{x}'_{l'}, \mathbf{q}) = -(k_B T) Tr \tilde{\beta} \tilde{\boldsymbol{\sigma}} \cdot \hat{\mathbf{n}} \sum_n \int \frac{d\mathbf{k}}{\nu_{BZ}} G_o(\mathbf{x}_l, \mathbf{x}'_{l'}, \mathbf{k}, \mu + i\omega_n) \times \tilde{\beta} \tilde{\boldsymbol{\sigma}} \cdot \hat{\mathbf{n}} G_o(\mathbf{x}'_{l'}, \mathbf{x}_l, \mathbf{k} + \mathbf{q}, \mu + i\omega_n) \quad (4)$$

The integral is over the Brillouin zone with wave vectors  $\mathbf{k}$ ,  $\mathbf{q}$  and  $\mathbf{k} + \mathbf{q}$  within the Brillouin zone of volume  $\nu_{BZ}$ . The sum is over the fermionic Matsubara frequencies. The Green's function for the unperturbed, paramagnetic system containing the band structure effects is obtained via relativistic multiple scattering (Korringa-Kohn-Rostoker, KKR) theory [19]. We solve equation (3) using a direct method of matrix inversion. The full Fourier transform is then generated

$$\chi^{\hat{\mathbf{n}}}(\mathbf{q}) = (1/V) \sum_l \sum_{l'} e^{i\mathbf{q}\cdot(\mathbf{a}_l - \mathbf{a}'_{l'})} \times \int d\mathbf{x}_l \int d\mathbf{x}'_{l'} e^{i\mathbf{q}\cdot(\mathbf{x}_l - \mathbf{x}'_{l'})} \chi^{\hat{\mathbf{n}}}(\mathbf{x}_l, \mathbf{x}'_{l'}, \mathbf{q}, \theta, \varphi) \quad (5)$$

where  $V$  is the volume of the unit cell. Some aspects of the numerical methods used to evaluate equations (3-5) of this type can be found in [15]. Note that this expression for the non-interacting susceptibility can be shown to be formally equivalent to one of the familiar type

$$\chi_o^{\hat{\mathbf{n}}}(\mathbf{q}) \propto \int d\mathbf{k} \sum_{j, j'} \frac{|M(\mathbf{k}, \mathbf{k} + \mathbf{q}, \hat{\mathbf{n}})|^2 f_{\mathbf{k}, j}(1 - f_{\mathbf{k} + \mathbf{q}, j'})}{\varepsilon_{j'}(\mathbf{k} + \mathbf{q}) - \varepsilon_j(\mathbf{k})} \quad (6)$$

where  $j$  is an electronic band index,  $\varepsilon_j(\mathbf{k})$  a single electron energy,  $M$  is a matrix element and  $f_{\mathbf{k}, j} = f(\varepsilon_j(\mathbf{k}), \mu, T)$ , the Fermi Dirac function.

The important feature of the response function (equations 3-5), is its dependence on the direction of the magnetic field,  $\hat{\mathbf{n}}$ , which vanishes when relativistic, spin-orbit coupling effects are omitted. The direction,  $\hat{\mathbf{n}} = (\sin\theta\cos\varphi, \sin\theta\sin\varphi, \cos\theta)$  is defined by polar and azimuth angles  $(\theta, \varphi)$ . In an h.c.p system such as *Y* or *Sc*, if an external magnetic field is applied along the  $\hat{\mathbf{n}} = (0, 0, 1)$  direction, i.e. the *c*-axis, where  $(\theta, \varphi) \rightarrow (0, 0)$ ,  $\chi_o^z$  is produced. On the other hand  $\chi_o^x$  is the response of the system when the field is applied in the *ab*-plane,  $\hat{\mathbf{n}} = (1, 0, 0)$ , and  $(\theta, \varphi) \rightarrow (\pi/2, 0)$ . We obtain an anisotropy as the difference in the non-interacting susceptibility when an external magnetic field is applied in two directions with respect to the crystal axes, i.e.  $(\chi_o^{\hat{\mathbf{n}}} - \chi_o^z)$ . This is enhanced by exchange and correlation effects (eq.3). The approach presented here is applicable to ordered compounds and elemental metals and can be modified to study disordered alloys [15] owing to its KKR multiple-scattering framework. In order to gauge the importance of these relativistic effects with atomic number, we compare our calculations of the magnetic response of *Y* with its lighter 3d counterpart *Sc*.

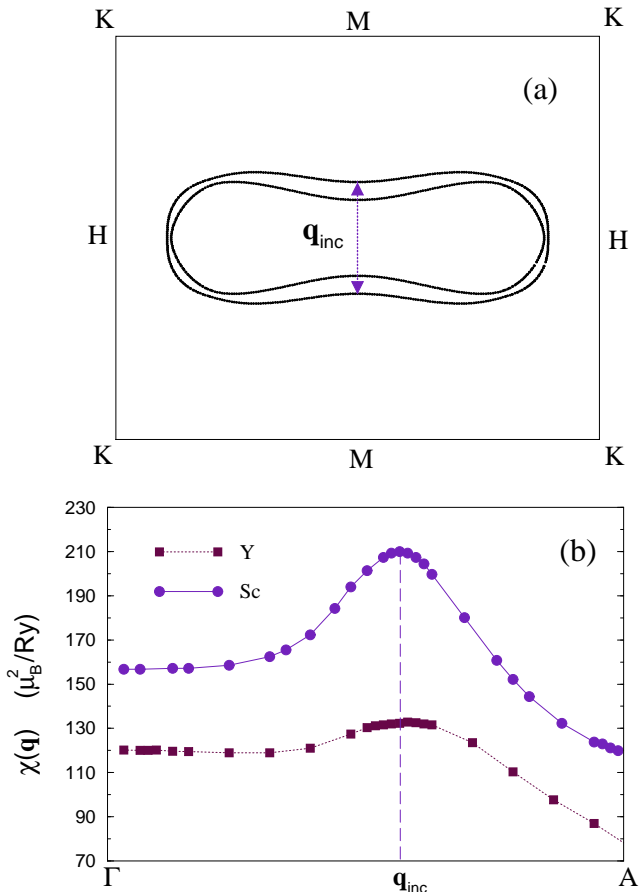


FIG. 1: (a) Cross-section of the ‘webbing’ Fermi surface in the H-L-M-K plane for Y. The nesting vector is indicated by the arrow. The special point L lies at the centre. (b) The enhanced susceptibility for Y and Sc along the  $\Gamma$ -A direction for  $T = 100\text{K}$ .

We use atomic sphere approximation (ASA), effective one-electron potentials and charge densities in the calculations for Y and Sc with experimental lattice constants  $a = 6.89$ ,  $c = 10.83$  and  $a = 6.24$ ,  $c = 9.91$  respectively, in atomic units,  $a_0$ . [20] The details of the electronic structures using a fully relativistic KKR method compare well with those from full potential calculations. [21] The Fermi surface for Y in the H-L-M-K plane is shown in Fig. 1(a). It shows two relatively flat parallel sheets. The nesting vector  $\mathbf{q}_{inc} = \pi/c(0,0,0.57)$  is indicated by the arrow. Fig. 1(a) is in very good agreement with previous calculations [3] and experiments [8, 22]. Dugdale *et al.* [8] have recently carried out positron annihilation fermiology experiments and measured  $\mathbf{q}_{inc} = \pi/c(0,0,0.55 \pm 0.02)$  for Y. Also, Vinokurova *et al.* [22], measured  $\mathbf{q}_{inc} \approx \pi/c(0,0,0.58)$ . We find a similar Fermi surface for Sc with the same nesting vector  $\mathbf{q}_{inc} = \pi/c(0,0,0.57)$ , also in good agreement with earlier calculations [23].

Our calculations of the enhanced static susceptibility, defined by equation (3), show a peak at this same wave-vector  $\mathbf{q}_{inc} = \pi/c(0,0,0.57)$  for both Y and Sc. This is

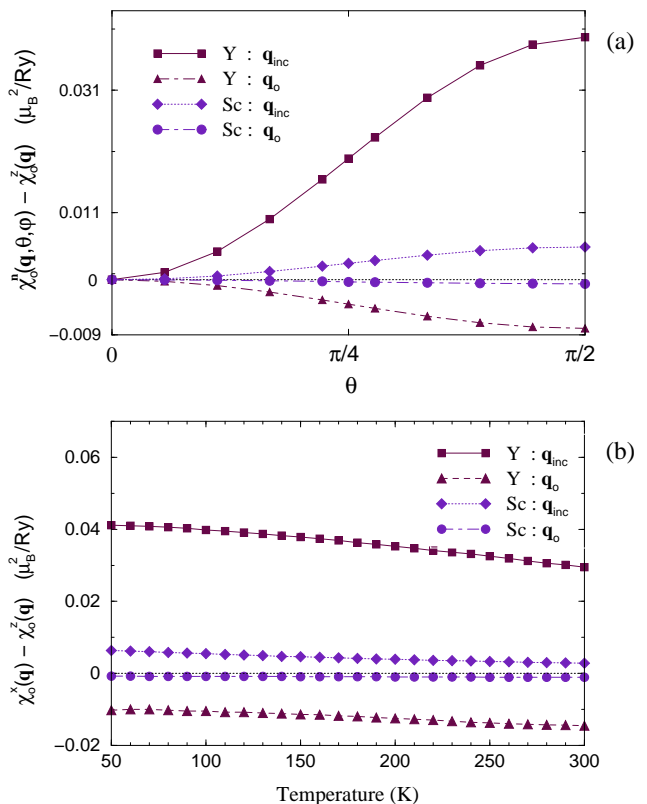


FIG. 2: (a) The anisotropy as a function of  $\theta$  for Y and Sc at  $\mathbf{q}_{inc} = \pi/c(0,0,0.57)$  and  $\mathbf{q}_o \simeq (0,0,0)$  and at  $T = 100\text{K}$ . (b) The temperature dependence of the anisotropy of Y and Sc at both the nesting vector  $\mathbf{q}_{inc}$  and  $\mathbf{q}_o$ .

shown in Fig. 1(b), where we probe wave-vectors along the  $c$ -axis from  $\Gamma$  to A. (The special point A, for h.c.p. crystal structures is  $(0,0,\pi/c)$ .) The temperature is set at 100K for these calculations.

Fig. 2(a) shows the anisotropy  $\chi_o^{\hat{\mathbf{n}}}(\mathbf{q}, \theta, \varphi) - \chi_o^z(\mathbf{q})$  as a function of  $\theta$  for Y and Sc at  $\mathbf{q}_{inc}$  and  $\mathbf{q}_o \simeq (0,0,0)$ . As expected on symmetry grounds, we find the anisotropy to be invariant in  $\varphi$ . This means that the magnetic response is insensitive to the direction along which an external magnetic field is applied in the  $ab$ -plane. As  $\theta$  is increased, an anisotropy is observed which reaches a maximum at  $\theta = \pi/2$  as shown in Fig. 2(a). In fact, we observe that the anisotropy takes the rather simple form

$$\chi_o^{\hat{\mathbf{n}}}(\mathbf{q}, \theta, \varphi) - \chi_o^z(\mathbf{q}) = (\chi_o^x(\mathbf{q}) - \chi_o^z(\mathbf{q})) \cdot |\hat{\mathbf{q}} \times \hat{\mathbf{n}}|^2 \quad (7)$$

for h.c.p. crystal structures [24] ( $|\hat{\mathbf{q}} \times \hat{\mathbf{n}}| = \sin \theta$ ). It is therefore sufficient to show  $\chi_o^x(\mathbf{q}) - \chi_o^z(\mathbf{q})$ , to determine the easy axes of the magnetic response. Fig. 2(b) shows the weak temperature dependence of the anisotropy of Y and Sc at both the nesting vector  $\mathbf{q}_{inc}$  and also at  $\mathbf{q}_o \simeq (0,0,0)$ . As expected, the anisotropy is an order of magnitude larger for Y than for Sc. This difference is a result of spin-orbit coupling being more pronounced in

the heavier 4d metal  $Y$  than in the 3d  $Sc$ . We infer that a still greater but similar anisotropy should be evident in the magnetic response of the conduction electrons in the heavier still RE materials.

It is apparent from Figs.1 and 2 that  $Y$  shows its strongest response at the wave-vector  $\mathbf{q}_{inc}$  which corresponds to the FS nesting and that the response here is strongest to magnetic fields directed in the basal  $ab$ -plane. Here, then, is an explanation as why  $Gd$  impurities, denoted typically as S ions (zero angular momentum) and thus free from crystal field effects, order into *helical* incommensurate AF states. [11] It is also a strong factor for the similar magnetic order found in other dilute rare-earth alloys such as  $Y Tb$ ,  $Y Dy$  and  $Y Ho$ . [10]

Fig.1(b) shows that yttrium's responses to ferromagnetic ( $\chi(\mathbf{q}) = (0,0,0)$ ) and  $\mathbf{q}_{inc}$ -AF modulations are close in strength. Figs.2(a) and 2(b) demonstrate, however, that the easy axis for a FM modulation lies along the  $c$ -axis and therefore contrary to that of the AF one. These features are pertinent to the magnetic structure of  $Gd - Y$  alloys. Pure gadolinium has a ferromagnetic phase with the easy axis along the  $c$ -axis so that in the paramagnetic phase at higher temperatures  $\chi(\mathbf{q})$  peaks at  $\mathbf{q} = (0,0,0)$ . Moreover its FS here has been observed not to possess a webbing feature [25]. Some recent experiments [25] have shown that adding more than around 30%  $Y$  to  $Gd$  changes the topology of the Fermi surface of the paramagnetic phase and the webbing is observed again. This is coincident with the alloys' forming helical AF states at lower temperatures. Moreover, in this concentration range, neutron-diffraction [9, 25] has shown that application of a modest uniform magnetic field along

the  $c$ -axis leads to a ferromagnetic alignment of the  $Gd$ -moments along the  $c$ -axis. Once the magnetic field is switched off the system reverts to its helical AF state. This suggests that the alloys'  $\chi(\mathbf{q})$ 's and anisotropies are similar to those shown in Fig.1(b) and Fig.2(a) but with the relative peak heights of  $\chi(\mathbf{q})$  at  $\mathbf{q} = (0,0,0)$  and  $\mathbf{q}_{inc}$  to be finely balanced.

In *conclusion*, we have described an *ab initio* theoretical formalism to calculate the relativistic static paramagnetic spin susceptibility for metals at finite temperatures. Since relativistic effects such as spin-orbit coupling are included we can identify the anisotropy or *easy axes* of the magnetic response. We applied this formalism to the 4d metal  $Y$ . Its enhanced susceptibility displays a peak at the incommensurate wave-vector  $\mathbf{q}_{inc} = (0,0,0.57\pi/c)$  traceable to a FS nesting feature found in the calculated electronic structure and fermiology experiments [8, 22]. The explanation of magnetic order in rare-earth- $Y$  alloys and superstructures in terms of the FS topology of  $Y$  is well established both on theoretical [4] and, more recently, experimental grounds. [8, 25] Results in this letter are fully consistent with these findings but we have also shown how the electronic structure of  $Y$  influences the canting of the rare earth moments with respect to the crystal axes. The finding that the incommensurate AF order of these moments has a helical structure whilst any potential ferromagnetism has an easy-axis parallel to the  $c$ -axis is suggested as a more general property of the conduction electrons of h.c.p. rare-earth materials and has a role in the magnetism of RE/ $Y$  multilayers.

We acknowledge support from the EPSRC (UK).

- 
- [1] T. Kasuya, in *Magnetism*, edited by G. T. Rado and H. Suhl (Academic Press Inc., New York, 1966), Vol. IIB, p. 215.
- [2] S. C. Keeton and T. L. Loucks, *Phys. Rev.* **168**, 672, (1968).
- [3] T. L. Loucks, *Phys. Rev.* **144**, 504, (1966).
- [4] S. H. Liu *et al.*, *Phys. Rev. B* **4**, 1100, (1971).
- [5] J. B. Staunton *et al.*, *J.Phys.:Cond. Mat.* **1**, 5157, (1989).
- [6] C.F.Majkrzak *et al.*, *Adv.Phys.* **40**, 99, (1991).
- [7] Y.Yafet, *J.Appl.Phys.* **61**, 4058, (1987).
- [8] S. B. Dugdale *et al.*, *Phys. Rev. Lett.* **9**, 941, (1997).
- [9] S.Bates *et al.*, *Phys. Rev. Lett.* **55**, 2968, (1985); R. J. Melville *et al.*, *J. Phys.: Cond. Mat.* **4**, 10045, (1992).
- [10] H.R.Child *et al.*, *Phys.Rev.* **138**, A1655, (1965); R. Cauldron *et al.*, *Phys. Rev. B* **42**, 2325, (1990).
- [11] N. Wakabayashi *et al.*, *Phys. Rev. B* **10**, 2049, (1974); P.J.Brown *et al.*, *J.Phys.Lett.* **46**, L1139, (1985); L.E.Wenger *et al.*, *Phys. Rev. Lett.* **56**, 1090, (1986).
- [12] A. K. Rajagopal and J. Callaway, *Phys. Rev. B*, **7**, 1912, (1973); A. H. MacDonald and S. H. Vosko, *J. Phys. C: Solid State Phys.* **12**, 2977, (1979).
- [13] S. H. Vosko and J. P. Perdew, *Can. J. Phys.* **53**, 1385, 1975.
- [14] A. H. MacDonald and S. H. Vosko, *J. Low Temp. Phys.* **25**, 27, 1976; A. H. MacDonald *et al.*, *Solid State Commun.* **18**, 85, 1976; M. Matsumoto *et al.*, *J. Phys.: Cond. Mat.* **2**, 8365, 1990.
- [15] J. B. Staunton *et al.*, *Phys. Rev. Lett.* **82**, 3340, (1999); J. B. Staunton *et al.*, *Phys. Rev. B*, **62**, 1075, (2000).
- [16] E. Stenzel *et al.*, *J. Phys. F* **16**,1789, (1986); S. Y. Savrasov, *Phys. Rev. Lett.* **81**, 2570, (1998).
- [17] A.L.Fetter and J.D.Walecka, 'Quantum Theory of Many Particle Systems', (McGraw-Hill), (1971).
- [18] U. von Barth and L. Hedin, *J. Phys. C* **5**, 1629, (1972).
- [19] J. S. Faulkner and G. M. Stocks, *Phys. Rev. B* **21**, 3222, (1980); P. Strange *et al.*, *J. Phys.:Condens.Mat* **1**, 2959, 1989.
- [20] *Pearson's Handbook of Crystallographic Data for Intermetallic Phases*, (American Society for Metals, Metals Park,OH,1985).
- [21] P. Blaha *et al.*, *Comput. Phys. Comm.* **59**, 399 (1996).
- [22] L. I. Vinokurova *et al.*, *JETP Lett.*, **34**, 566, (1981).
- [23] G. S. Flemming and T. L. Loucks, *Phys. Rev.* **173**, 685, (1968).
- [24] We also find this relationship to hold for tetragonal crystal structures.
- [25] H. M. Fretwell *et al.*, *Phys. Rev. Lett.* **82**, 3867, (1999).